Evolution of the mass-loss rate during atmospheric and pressurized slow pyrolysis of wheat straw in a bench-scale reactor

Gianluca Greco[a], María Videgain[a], Christian Di Stasi[a], Belén González[a], Joan J. Manyà[a,b,*]

[a] *Technological College of Huesca,* [b] *Aragón Institute of Engineering Research (I3A), University of Zaragoza, crta. Cuarte s/n, Huesca E-22071, Spain*

[*] Corresponding author. E-mail address: joanjoma@unizar.es.

HIGHLIGHTS

- Higher pressure led to higher devolatilization rates in a narrower period of time
- Using a mixture of CO_2 and N_2 at 0.1 MPa favored the thermal cracking of volatiles
- Under CO_2/N_2 an increased pressure led to a decrease in the yields of CO and CH_4
- Biochar produced at 0.1 MPa under CO_2/N_2 had the highest specific surface area

ABSTRACT

In the present study, the effects of the absolute pressure (0.1 or 0.5 MPa) and the reactor atmosphere (pure N_2 or a mixture of CO_2/N_2) on the pyrolysis behavior of wheat straw pellets (at 500 °C) were investigated. The most interesting aspect of this work was the use of a weighing platform (with a maximum capacity of 100 kg and a resolution of 0.5 g) to monitor the real-time mass-loss data for the biomass sample (with an initial mass of 400 g). It was observed that an increased pressure considerably affects the mass-loss profiles during the pyrolysis process, leading to higher devolatilization rates in a shorter period of time. Regardless of the pyrolysis atmosphere, an increase in the absolute pressure led to higher yields of gas at the expense of produced water and condensable organic compounds. This finding could be due to the fact that an increased pressure favors the exothermic secondary reactions of the intermediate volatile organic compounds in both liquid and vapor phases. The switch from pure N_2 to a mixture of CO_2 and N_2 at 0.1 MPa also led to a remarkable increase in the yield of produced gas at the expense of the total liquid. This could be mainly due to the promotion of the thermal cracking of the volatile organic compounds at a high partial pressure of CO_2, which is also consistent with the measured higher yields of CH_4 and CO. The increased yield of CO can also be seen as a direct result of the enhanced reverse Boudouard reaction, which can also explain the much higher specific surface area (and ultra-micropore volume) measured for the biochar produced under the same operating conditions (0.1 MPa and a mixture CO_2/N_2 as pyrolysis medium).

KEYWORDS

Wheat straw; Pyrolysis; Biochar; CO_2 atmosphere; Pressure; Devolatilization rate

1. Introduction

The energy crisis, environmental pollution and global warming are serious problems, which have recently generated a growing interest in developing new technologies focused on reducing the greenhouse gas emissions and increasing the carbon sinks [1]. A promising solution for such issues is biochar [2], a form of charred organic matter, which is possible to apply to soil in a deliberate manner as a means of potentially improving soil productivity and carbon sequestration [3]. In order to produce biochar, pyrolysis of agricultural wastes seems to be an interesting solution, due to its feasibility to manage biowaste and simultaneously generate environmental and agronomic benefits [4,5]. Among the wide range of pyrolysis processes, slow pyrolysis is a promising route to produce a relatively high yield of biochar, obtaining gas as co-product for cogeneration use. This process, which is carried out at low heating rates and long residence times of both the solid and vapor phases [6], is relatively simple and robust and can be feasible for small-scale and farm-based production of biochar [7]. Given the high number of variables affecting the process (such as peak temperature, heating rate, gas residence time, and pressure) and the wide range of available biomass sources, (the nature of which largely affects the pyrolysis process) a large variability in the yield and properties of the produced biochar should be expected. Therefore, one of the main challenges nowadays is to optimize the process conditions of the pyrolysis process for a given biomass feedstock [8,9] with the aim to obtain an engineered biochar with the desired properties to be used for a given application. Regardless of the final use of the produced biochar (e.g., soil amendment, material precursor for activated carbons), the assessment of the stability of biochar's carbon appears to be essential in order to evaluate its potential as carbon sequestration agent.

Among all the process variables, the absolute pressure is probably one of the most interesting parameters to study in deep. Relatively few studies [4,10–16] have been focused on the effect of the absolute pressure on the biomass pyrolysis behavior. Most of these earlier studies reported an increase in the char and gas yields, while the yield of the condensable fraction decreased, when both the pressure and the residence time of the vapor phase were increased [13,15–19]. Nevertheless, some

authors found a negligible [20] or even a negative [10,21] effect of the absolute pressure on the char yield. For instance, Manyà et al. [10], who analyzed the effect of the absolute pressure (in the range of 0.1–1.0 MPa) on the pyrolysis of two-phase olive mill waste in a laboratory-scale fixed-bed reactor (keeping constant the residence time of the vapor phase within the reactor by adjusting the mass flow rate of the inert gas), already observed a significant decrease in the char yield when the pressure was increased. This finding suggested that the real effect of pressure (i.e., without interaction of the residence time of the vapor phase) was really complex, since an increased pressure could lead to an enhancement of the kinetics of the steam gasification reaction, which might be further explained by the catalytic effect of the alkali and alkaline earth metal species (AAEMs) present in the biomass feedstock. Therefore, the effect of the absolute pressure on the pyrolysis behavior of any feedstock has not been properly demonstrated yet.

Another important parameter affecting the pyrolysis behavior is the type of carrier gas used to maintain oxygen-free conditions [5]. In terms of energy efficiency, the flue gas generated by combustion of pyrolysis gas can be used as pyrolysis gas environment. This approach, which can lead to important cost savings [22], may be suitable in small-scale and farm-based systems, resulting in an improvement in the biochar production process in terms of economic feasibility, environmental impact, and thermal efficiency. Nevertheless, further research is needed to analyze the effects of modifying the inert environment (i.e., from pure N_2 to a flue gas containing CO_2) on the pyrolysis products distribution as well as on the biochar properties.

As mentioned above, special attention should also be paid to those properties of biochar that are related to its carbon sequestration potential. For this purpose, the fixed-carbon content and the atomic H:C and O:C ratios appear as useful rough indicators of the long-term stability of biochar's carbon [9,23–26]. In fact, a recent publication [25] reported that the above-mentioned indicators exhibited a strong correlation with both the recalcitrance index (R_{50}) [27] and the *stable-C* [28], which are based on the relative thermal stability of a given biochar to that of graphite (R_{50}), and on oxidation of biochar using H_2O_2 to accelerate the oxidative loss of carbon (*stable C*).

The specific aim of this study is to analyze the effect of both the absolute pressure (0.1 or 0.5 MPa) and the type of pyrolysis atmosphere (pure N_2 or a binary mixture of CO_2 and N_2, 60:40 v/v), at a constant peak temperature of 500 °C, on the pyrolysis behavior of wheat straw pellets in a pressurized fixed-bed reactor. The pyrolysis device is equipped with a weighing platform, which was employed to monitor the real-time mass loss of the biomass along the pyrolysis process. To the best of our knowledge, this is one of the first studies using a bench-scale reactor coupled to a weighing platform. This approach can provide very useful insights to better understand the pyrolysis behavior at a relatively large scale (compared to traditional TGA or even macro-TGA measurements), where the secondary reactions of primary volatiles play a key role. The simultaneous analysis of the real-time mass-loss data, gas composition, and temperature profiles can provide a unique way to assess the role played by the studied factors (pressure and pyrolysis atmosphere) on the pyrolysis process.

2. Experimental Section

2.1. Biomass feedstock

The wheat straw (WS) pellets (7 mm OD and approximately 12 mm long) used in this work were supplied by a Belgian company. No binder was used in making the pellets. WS pellets were directly pyrolyzed without any preliminary milling step. The reason is that the efficiency of carbonization can be improved for large particles as compared with small ones, leading to charcoals with higher fixed-carbon contents [24,29].

Proximate analysis was performed in quadruplicate according to ASTM standards (D3173 for moisture, D3174 for ash, and D3175 for volatile matter), whereas ultimate analysis was carried out in triplicate using a combustion elemental analysis Leco CHN628 (Leco Corporation, USA). In addition, X-Ray Fluorescence (XRF) spectroscopy analysis (ADVANT'XP+ XRF spectrometer from Thermo ARL, Switzerland) was performed in order to determine the inorganic constituents of the biomass ash.

A thermogravimetric analyzer (Netzsch 449 F1 Jupiter) was used to obtain the pyrolysis thermogravimetric curves (at a heating rate of 10 K min^{-1} and a final temperature of 800 °C) under an environment of pure N_2. The initial mass of sample was 10 mg. In order to roughly estimate the contents of the main biomass constituents, the experimental differential thermogravimetric (DTG) curve was deconvoluted into three peaks using the "Peak Analyzer" tool implemented in OriginPro version 9.0 (OriginLab, USA). These three peaks can be associated to the devolatilization of hemicelluloses plus extractives (peak 1), cellulose (peak 2), and lignin (peak 3) [25].

2.2. Pyrolysis device and experimental procedure

Pyrolysis runs were conducted in duplicate in a bench-scale fixed-bed reactor. Fig. 1 shows the scheme of the experimental device, the details of which are available in a previous study [5]. Briefly, the reactor (140 mm ID and 465 mm long) was made of Sandvik 253 MA stainless steel (EN 1.4835). A basket of 4 L, made of AISI 316 (EN 1.4401) stainless steel wire mesh, was used to allocate the biomass into the reactor. The initial sample weight was approximately 400 g, which represented around 30% of the basket volume. A weighing platform from Kern (model DS with a measuring range up to 100 kg and a reading precision of 0.5 g) was placed at the bottom of the reactor system. A ceramic tube (117 mm OD and 330 mm long) was positioned between the reactor vessel and the weighing platform for thermal insulation purposes. Flexible stainless-steel tubing from Swagelok (10 mm OD) were used for the reactor connections to minimize any force component.

As widely reported in literature [7,8,10,30–34], higher pyrolysis temperatures usually led to lower biochar yields, hydrogen and oxygen contents, and aliphatic carbon fraction. In other words, increasing peak temperature results in more potentially stable biochars. However, it is interesting to find a compromise between yield and potential stability. In this sense, a previous study [35] showed that pyrolysis peak temperatures higher than 500 °C could be enough to obtain a biochar with an appropriate content of stable polycyclic aromatic carbon. Moreover, our previous experience with other biomass sources [25] indicated that higher temperatures (e.g., 600 °C) did not necessarily lead

to a further improvement in the potential stability of biochar. Therefore, a peak temperature of 500 °C was selected as a reasonable trade-off between the biochar yield and its potential stability and was kept constant for all the pyrolysis runs.

In the present study, the experimental factors to consider were the absolute pressure (0.1 or 0.5 MPa) and the type of carrier gas (pure N_2 or a mixture of CO_2 and N_2, 60:40 v/v). The real flow rate of the carrier gas within the reactor at 500 °C was kept constant at 3.24 L min^{-1}, regardless of the pressure applied, by properly adjusting the mass flow rate. Assuming an entire reactor's void-volume fraction of 0.9, the above-mentioned flow rate corresponds to a gas-hourly space velocity (GHSV) of 36 h^{-1}. This approach is interesting in order to assess the effect of the absolute pressure instead of the combined effect of the absolute pressure plus the pressure-dependent gas residence time.

Temperature inside the bed was measured by four thermocouples located in a thermowell (placed at a radial distance of 35 mm from the axis) at different heights from the bottom of the sample basket: 10 mm (TC_0), 50 mm (TC_1), 200 mm (TC_2), and 300 mm (TC_3). During the course of the pyrolysis runs, the sample was heated at an average heating rate of 5 °C min^{-1} to reach the peak temperature (500 °C). Due to the fact that a certain thermal gradient can exist along the packed bed, the average temperature of the two thermocouples placed at the bottom of the bed (TC_0 and TC_1) was chosen as the main process temperature. A soaking time of 60 min (at the peak temperature) was chosen to ensure the thermal equilibrium.

A back-pressure regulator was used to maintain the pressure of the system at a desired value. The outlet gas stream passed through a heated line, maintained at a temperature of around 375 °C, before being passed through a series of glass traps, which were immerged in ice-water baths. After each experiment, the biochar produced was collected and weighted. The glass traps were weighted before and after each pyrolysis run to estimate the total mass of liquid (water + organics). The pyrolysis liquid was recovered directly from the condensers without using any solvent as wash liquid. The water content of the pyrolysis liquid was then determined by Karl Fischer titration, while the yield of organic compounds was determined by difference from the total mass of liquid.

The composition of the major components of the pyrolysis gas (N_2, CO_2, CO, CH_4, C_2H_X and H_2) was determined using a micro gas chromatograph (μ-GC, Agilent 490) equipped with two analytical columns: a Molsieve 5A (using Ar as carrier gas) and a PolarPlot U (using He as carrier gas). The mass of produced gas was estimated from the N_2 mass balances.

In order to correct the buoyancy and other thermal expansion effects, blank tests (i.e., empty reactor) at 0.1 and 0.5 MPa were carried out employing the same heating program as for the experiments with biomass. The real-time mass loss for a given pyrolysis test was then obtained by subtracting the blank measurement from the raw signal.

2.3. Characterization of the pyrolysis products

The mass yield of biochar (y_{char}), volatile organic compounds (y_{org}), produced water (y_{water}) and produced gas (y_{gas}) were calculated on a dry and ash-free (daf) basis. Biochar samples were characterized by both proximate and ultimate analyses following the same procedures as described in Section 2.1. The carbonization efficiency was assessed by determining the fixed-carbon yield (y_{FC}), similarly to how it was done in previous studies [10]:

$$y_{FC} = x_{FC,bc}\, y_{char} \tag{1}$$

where $x_{FC,bc}$ is the mass fraction of fixed-carbon in the biochar (calculated in a dry and ash-free basis). The value of y_{FC} corresponds to the fraction of organic matter initially present in the biomass feedstock that is converted into fixed carbon.

Due to the highly microporous structure of biochar, specific surface areas (S_{BET}) were determined from the CO_2 adsorption isotherms at 0 °C [36], which were obtained using an ASAP 2020 gas sorption analyzer from Micromeritics (USA). Samples (around 120–200 mg) were previously degassed under dynamic vacuum conditions to constant weight at 150 °C. Pore size distributions (from 0.35 to 1.0 nm) and the ultra-micropore volume (V_{ultra}, for pore sizes lower than 0.8 nm) of biochars were estimated using a Grand Canonical Monte Carlo (GCMC) method for carbon slit-

shaped pores. All the calculations from CO_2 adsorption isotherms were performed using the MicroActive software supplied by Micromeritics.

3. Results and discussion

Table 1 shows the results pertaining to the characterization of the wheat straw pellets (proximate, ultimate, and XRF analysis). From the results concerning the inorganic constituents, it should be highlighted the high amount of K and Ca (AAEMs). Hence, a certain catalytic role of them should be expected in this study.

The mass-balance closures for the pyrolysis tests were estimated to be within 91%−99% (see Table S1 in the Supplementary Data). The mass yields of the different pyrolysis products (y_{char}, y_{water}, y_{org} and y_{gas}) were calculated attributing the error in the mass-balance closure to minor inaccuracies in determining the mass of produced gas. As each experimental run was conducted in duplicate, the mass yields of the pyrolysis products correspond to the average values.

With regard to the accuracy of the obtained mass-loss curves, we assessed the repeatability of three blank tests (two at 0.1 MPa and one at 0.5 MPa) as well as four pyrolysis runs (at 0.1 MPa and using a mixture of CO_2 and N_2 as carrier gas). The results from the three blank tests (see Fig. S1) indicated a reasonable degree of repeatability. Also according to Fig. S1, pressure had a negligible effect on the blank mass-loss curve. Therefore, we took the average from the three replicates as the blank signal to be subtracted from the raw mass-loss curves. For its part, Fig. S2 displays the results obtained from the four repeated pyrolysis runs. As can be seen from Fig. S2, a more than acceptable degree of repeatability was reached (see also explanatory notes for Fig. S2 in the Supplementary Data).

3.1. Pyrolysis behavior

Fig. 2 shows the mass-loss profiles obtained for the four pyrolysis runs: at 0.1 and 0.5 MPa under pure N_2 (0.1_N_2; 0.5_N_2) in Fig. 2a; and at 0.1 and 0.5 MPa under the mixture CO_2/N_2 (0.1_N_2&CO_2; 0.5_N_2&CO_2) in Fig. 2b. A certain level of noise can be seen in the mass loss plots. This noise is difficult to avoid in practice, since several factors such as the room temperature (small changes of

which could slightly alter the weight measurement due to the extreme sensitivity of the scale), small changes in the heating program, and the exact position of the reactor inside the furnace could markedly affect the stability of the acquired signal over time. However, the plots displayed in Fig. 2 provide a very interesting information for the purpose of the present work. As expected, two mass-loss steps are clearly shown in Fig. 2. The first one corresponds to the evaporation of the moisture fraction of the feedstock, whereas the second one is the mass loss due to the devolatilization process at 180–500 °C.

To better visualize the effects of the studied factors on the pyrolysis behavior, Fig. 3 simultaneously displays the time derivative of the mass loss, the evolution of temperature within the bed (TC_0 and TC_1), and the molar flows of the main gaseous species released during the pyrolysis process (produced CO_2, CO, CH_4, and H_2). The detailed location of the four thermocouples and the obtained axial temperature profiles (for all thermocouples) are shown in Figs. S3 and S4, respectively. The plots in Fig. S4 clearly show severe axial temperature gradients throughout the reactor, especially for the thermocouples located outside the packed bed (TC_2 and TC_3). For pyrolysis runs performed at 0.5 MPa, the temperature gradients slightly decreased (i.e., higher values were recorded by thermocouples TC_2 and TC_3), probably as a consequence of the enhanced convective heat transfer related to the higher N_2 mass flow rate. Nevertheless, no large differences in the temperatures measured by TC_0 and TC_1 (both located within the bed) were found. This could confirm a relatively homogeneous heating throughout the bed length.

In light of the shape of the time derivatives of the mass loss shown in Fig. 3, it can be pointed out that the absolute pressure greatly affected the release of volatiles during the pyrolysis process. At 0.5 MPa, and regardless of the pyrolysis atmosphere, higher devolatilization rates in a narrower period of time, compared to the two experiments conducted at 0.1 MPa, were clearly observed. Regarding the position of the mass-loss peaks, the temperatures at which the highest devolatilization rate was attained (T_{max}) were: 263 °C (0.1_N_2), 339 °C (0.5_N_2), 300 °C (0.1_N_2&CO_2), and 261 °C (0.5_N_2&CO_2). Therefore, the values of T_{max} seem to depend on both the absolute pressure and the

pyrolysis atmosphere. Unexpectedly, these temperature values were relatively similar and, in the most of cases, even lower than that deduced from the thermogravimetric analysis (around 325 °C, as can be deduced from the DTG curve shown in Fig. S5). Considering the heat transfer limitations existing in our fixed-bed reactor system, this unexpected result could be due to the presence of large radial temperature gradients. In other words, the temperatures registered by the thermocouples could correspond to the lowest (or almost lowest) temperature values in the bed at a given time. In the next subsections, further discussion is provided for each of the two different pyrolysis atmospheres.

3.1.1. Pure N_2 atmosphere

It is generally assumed that an increase in the absolute pressure could lead to a promotion of the secondary cross-linking reactions at relatively low temperatures (i.e., lower than T_{max}), as a consequence of the restricted release of volatiles [25,37]. This fact can explain the observed behaviors when the pyrolysis atmosphere was pure N_2: an increase in T_{max} with pressure and, as shown in Fig. 4a, an increase in the yield of produced gas (y_{gas}) at the expense of both the produced water (y_{water}) and, to a lesser extent, the condensable organic compounds (y_{org}). The yield of biochar, however, was kept almost constant, regardless of the pressure applied. This can suggest that an increased pressure results in a double effect: (1) a higher pressure (probably combined with the catalytic role of the AAEM species) can enhance the release of volatiles (once they reach the increased saturation temperature), leading to a higher devolatilization rate at higher temperatures; and (2), and as mentioned above, a higher pressure can also promote the secondary charring reactions (especially at intra-particle level and at relatively low temperatures) and simultaneously favor the thermal cracking and steam reforming of intermediate volatile organic compounds, leading to a decrease in the cumulative yield of the total liquid (mainly water) at the expense of produced gas and biochar.

The observed decrease in the yield of produced water with pressure, which was also reported by Ates et al. [38] for the pressurized pyrolysis of two biomass sources, seems to be contradictory with the higher extent of the secondary reactions of the primary volatile species, since both thermal cracking and dehydration processes can notably increase the production of water [19]. However, a

higher consumption of water can also be promoted by pressure by means of an enhancement of several reactions: (1) steam reforming of volatile organic compounds and/or light hydrocarbons, (2) water-gas-shift reaction (reaction #1 in Table 2), and (3) steam gasification (reaction #5 in Table 2). Despite the fact that secondary reactions of primary volatiles could mainly explain the obtained product yields, a certain role of the theoretical reactions listed in Table 2 cannot be ignored, since the residence time of permanent gases within the reactor is quite long (around 100 s assuming a GHSV of 36 h^{-1}). In this sense and as already observed in previous studies [4,10], a low (but certain) extent of the steam gasification reaction cannot be discarded. In spite of the extremely low temperature and the related thermodynamic limitations, the AAEMs contained in the wheat straw pellets (especially K, with a relatively high content, as reported in Table 1) can enhance the kinetics of the reaction, especially at 0.5 MPa. This can also partly explain the almost constant yield of biochar regardless of the pressure applied. In other words, a certain consumption of carbon via steam gasification can compensate the additional char produced through secondary charring reactions of the primary volatiles.

Fig. 3 also shows that the absolute pressure caused a certain effect on the evolution of the two temperatures inside the bed (TC_0 and TC_1). Both temperatures just increased up to approximately 500 °C (the selected peak temperature) at 0.1 MPa, showing the highest heating rate in correspondence with the highest devolatilization rate. However, when the pressure was set at 0.5 MPa, the two temperatures increased along the process, showing a heating rate (during the devolatilization step) faster than that observed at atmospheric pressure. This is consistent with the higher extent of the above-mentioned secondary reactions, which have an exothermic nature. The observed slight decrease in temperature (of about 30 °C, just after attaining the highest devolatilization rate) for pressurized experiments can be explained by a transient response of the PID controller (i.e., a lower power was supplied to the furnace during a relatively short period).

Concerning the gas release profiles (also shown in Fig. 3), it can be seen that CO_2 and CO were the first gases to be released in all the cases, showing a peak at approximately the value of T_{max} (263 °C and 339 °C at 0.1 and 0.5 MPa, respectively; see Fig. 3a), followed by the generation of CH_4 and

H_2 at considerably higher temperatures. The production of CO_2 and CO at relatively low temperatures was mainly due to the thermal decomposition of hemicelluloses and extractives, in particular to their decarboxylation and decarbonylation reactions. Fig. S6 shows that the percentage of area corresponding to the first peak (attributed to the decomposition of hemicelluloses and extractives) was 52.5%. Further release of CO_2 and CO at higher temperatures can be attributed to the decomposition of cellulose (with a related second peak representing 27.8% of the total area). For its part, the release of CH_4 (which is partly due to the decomposition of lignin) occurred at temperatures in the range of 375−450 °C. As can be seen in Figs. 4a−b, two different peaks in the release of CH_4 can be distinguished: the first one (at lower temperature) could correspond to the decomposition of lignin, whereas the second one (more pronounced at 0.5 MPa) may be due to a subsequent cracking of volatiles and/or the promotion of some methanation reaction in gas phase. Regarding the H_2 release profile, it should be highlighted that the most part of which appeared when the main devolatilization step was already concluded. Given the fact that the mass-loss profile did not show any considerable change during the highest release of H_2, we can suggest that the formation of H_2 can mainly be attributed to secondary homogeneous gas-phase reactions.

Fig. 5a displays the cumulative yields of the main gaseous species (in mmol g^{-1} of feedstock in a daf basis) for the experiments conducted under a pure N_2 environment. All the yields notably increased when a pressure of 0.5 MPa was applied, partly as a result of the higher extent of secondary pyrolysis reactions, leading to a higher production of permanent gases from intermediate volatile organic compounds. This fact could explain the higher peaks observed in Fig. 3b (compared with those of Fig. 3a) for CO_2, CO and CH_4 during the devolatilization process (i.e., when the mass loss of biomass still continued). However, and as has been pointed out before, an additional formation of CH_4 at higher temperatures (i.e., the second peak of CH_4) is clearly enhanced at 0.5 MPa. From a thermodynamics point of view, the additional formation of CH_4 can be explained by an enhancement of methanation reactions (see reactions #3, #4, and #6 in Table 2). For its part, the higher production of CO_2 at 0.5 MPa could be explained by the promotion of reactions #2 (Boudouard) and #6 (reverse

dry reforming). Nevertheless, the fact that the yield of CO also increased with pressure (in spite of its consumption through reactions #2, #3, and #6) suggests that further reactions are involved. One of them could be the above-mentioned steam gasification reaction (reaction #5 in Table 2), which can also partly explain the decreased yield of produced water at high pressure.

3.1.2. CO_2/N_2 atmosphere

Using a carrier gas composed of a mixture of CO_2 and N_2 (60:40 v/v) led to considerable changes in the pyrolysis behavior (as compared with that observed using pure N_2) at both 0.1 and 0.5 MPa. At atmospheric pressure, a higher exothermicity during the main devolatilization stage can be observed in Fig. 3c (in comparison to the temperature profiles at 0.1 MPa shown in Fig. 3a), leading to a higher value of T_{max} (300 °C instead of 263 °C). This observed higher exothermic behavior might be explained by a promotion of the secondary reactions of the primary volatile organic compounds. This finding is in agreement with a recent study focused on slow pyrolysis of red pepper stalk [39], in which the observed decrease in tar yield (in favor of produced gas) was attributed to an enhancement of the thermal cracking of volatiles when an atmosphere of CO_2 was used. Interestingly and as can be seen in Fig. 4b, the yield of biochar (y_{char}) was almost the same than that obtained using pure N_2 at 0.1 MPa. In fact, the higher yield of produced gas (under an atmosphere of CO_2/N_2) was at the expense of the total production of liquid ($y_{water} + y_{org}$). The fact that the yield of produced water also decreased at 0.1 MPa, using a pyrolysis environment composed of a mixture of CO_2 and N_2, can suggest that CO_2 also promotes the further consumption of water through steam reforming and/or steam gasification reactions.

Regarding the yields of the main gaseous species obtained at 0.1 MPa (see Fig. 5b), it should be highlighted the higher yields of CO and CH_4 compared with those measured using an atmosphere of N_2. The increase in the yield of CH_4 (1.02 mmol g^{-1}, 86% higher than that using N_2), as well as in the yield of C_2 hydrocarbons ($C_2H_4 + C_2H_6$), could be related to the above-mentioned higher extent of the thermal cracking of volatile organic compounds [39]. In the case of the yield of CO (2.73 mmol g^{-1}, 127% higher than that using N_2 at 0.1 MPa), its increase could be due to different chemical

processes: (1) thermal cracking of intermediate volatile compounds (such as carboxylic acids and phenolic compounds), (2) reverse water-gas-shift reaction, which is thermodynamically promoted and probably further enhanced by the relatively high partial pressure of CO_2, and (3) reverse Boudouard reaction, which can also be promoted by the high concentration of CO_2, despite the fact that this reaction is thermodynamically disfavored and extremely slow at the temperatures used here.

As expected, a further increase in the yield of produced gas at the expense of the yield of liquid ($y_{water} + y_{org}$) was observed when pressure raised to 0.5 MPa (see Fig. 4b). Nevertheless, the yields of gaseous species did not follow the expected trend. Fig. 5b shows a notably decrease in the yields of CO and CH_4 compared with those obtained at 0.1 MPa using a mixture of CO_2 and N_2. In other words, and unlike the trend observed for the pyrolysis experiments conducted in a pure N_2 environment, an increased pressure did not lead to any improvement in the pyrolysis gas composition when CO_2 was used as carrier gas. The observed increase in the yield of CO_2 (5.72 mmol g^{-1}, 31% higher than that using CO_2/N_2 at 0.1 MPa, and 15% higher than that using N_2 at 0.5 MPa) could be explained by a promotion of the Boudouard reaction at 0.5 MPa. A further evidence supporting this assumption is the observed decrease in the yield of CO (y_{CO}) when the absolute pressure was increased under a pyrolysis atmosphere of CO_2/N_2: from 2.73 mmol g^{-1} at 0.1 MPa to 2.14 mmol g^{-1} at 0.5 MPa. Furthermore, the CH_4 yield also decreased at 0.5 MPa (0.709 mmol g^{-1}, 30% lower than that using CO_2/N_2 at 0.1 MPa). This finding could be related to a certain enhancement of the dry reforming of CH_4 (reverse reaction #6 in Table 2), due to the high partial pressure of CO_2 [22,40].

The observed deterioration in the quality of the produced gas (at 0.5 MPa using a mixture of CO_2 and N_2) seems to be in disagreement with previous studies [5,25], in which an improvement in the pyrolysis gas (in terms of yield of CO and heating value) was reported when pyrolysis of biomass (vine shoots, olive mill waste, and corn stover) at a peak temperature of 600 °C was conducted at 1.0 MPa under an atmosphere composed of pure [5] or almost pure (95% vol. [25]) CO_2. However, the discrepancies in the results can be explained by differences in the pyrolysis peak temperature (500 °C in the present study), and, to a lesser extent, partial pressure of CO_2 (which is lower here), and the

biomass feedstock (having different contents of ash and different inorganic constituents). In this sense, the lower pyrolysis temperature used in the present study can lead to very different rates and extents of the involved reversible reactions.

3.2 Biochar properties

The main characteristics of the biochars produced under different operating conditions are reported in Table 3. The biochar having the highest fixed-carbon content (70.0% in dry basis, 79.3% in daf basis) was obtained under pure N_2 at 0.5 MPa. Given that the yields of biochar were practically the same, regardless of the pyrolysis conditions, the carbonization efficiency was also maximized at 0.5 MPa under an atmosphere of pure N_2 (y_{FC} = 0.231; approximately 15% higher than that for the rest of pyrolysis runs). This result can be attributed to the role of pressure in the promotion of secondary reactions. As mentioned in Section 3.1.1, an increased pressure can delay the transfer of volatiles into the vapor phase and thereby promote liquid-phase coking reactions that enhance the formation of fixed carbon [29]. However, an increased pressure did not lead to any improvement in the fixed-carbon yield when an atmosphere of CO_2/N_2 was used. One possible explanation can be related to the finding recently reported by Lee at al. [39], who observed a faster thermal degradation of lignin when CO_2 was used as pyrolysis medium instead of N_2. Given the fact that the content of lignin (in a given biomass feedstock) is directly correlated to the yield of fixed carbon [13], a higher degradation of this amorphous substance can lead to a lower fixed-carbon yield.

Concerning the atomic H:C and O:C ratios reported in Table 3, it should be pointed out that the values for all produced biochars were very low (0.44−0.54 and 0.04−0.09, respectively), in spite of the relatively low pyrolysis peak temperature (500 °C). For instance, Windeatt et al. [41] reported H:C ratio values in the range of 0.4−0.5 for biochars produced from several crop residues through atmospheric pyrolysis (under N_2) at a higher peak temperature of 600 °C. Furthermore, a slight decrease in the atomic ratios (at both 0.1 and 0.5 MPa) was observed when the pyrolysis atmosphere was a mixture of CO_2 and N_2. However, these differences (which can be within experimental error,

especially for the O:C ratio) are too small to be considered as improvement in the carbon sequestration potential. In fact, the biochar having the lowest H:C and O:C ratios (produced at 0.5 MPa and under CO_2/N_2) does not exhibit the highest fixed-carbon content. In other words, we cannot assume that using an atmosphere of CO_2/N_2 (instead of pure N_2) can lead to biochars with higher potential stability. This is consistent with the results from an earlier study [25], in which no significant statistical effects on the potential stability of biochar's carbon were observed for neither the absolute pressure (in the range of 0.1−1.0 MPa) nor the pyrolysis atmosphere (pure N_2 or a mixture CO_2/N_2 95:5 v/v).

Table 3 also lists the textural parameters deduced from the CO_2 adsorption isotherms at 0 °C (which are displayed in Fig. S7). In addition to the BET specific surface area (S_{BET}), the limiting micropore volumes from the Dubinin-Radushkevich equation (V_{DR}) and the ultra-micropore volume (V_{ultra}) are also reported in Table 3. Two considerations can be drawn from the reported textural parameters and the pore size distributions shown in Fig. 6: (1) under a pyrolysis medium composed of pure N_2, the microporosity development of biochars was not affected by the absolute pressure for the range of operating conditions tested in this study, and (2) using a mixture of CO_2/N_2 as pyrolysis environment at atmospheric pressure led to notably higher microporous biochars. The fact that the presence of CO_2 at 0.1 MPa favors the porosity development of biochars could be due to the promotion of the reverse Boudouard reaction under these conditions. This is consistent with the increased yield of CO, which we already mentioned in Section 3.1.2. It must be highlighted the high ultra-micropore volume (a key parameter for CO_2 adsorption capacity) measured for the biochar produced at 0.1 MPa under CO_2/N_2: 0.150 $cm^3\ g^{-1}$. This value is within the range or even higher than the ultra-micropore volumes reported for biomass-derived physically or chemically activated carbons [42,43]. Further research in this direction seems to be highly interesting to produce "low-temperature" carbon-based adsorbents for the selective removal of CO_2 in gas phase.

4. Conclusions

From the analysis of results presented above, the following main conclusions can be drawn:

(1) An increased pressure considerably affects the mass-loss profiles during the pyrolysis process, leading to higher devolatilization rates in a shorter period of time. Regardless of the pyrolysis atmosphere, an increase in the absolute pressure led to higher yields of produced gas at the expense of produced water and condensable organic compounds. This finding is related to the fact that an increased pressure favors the exothermic secondary reactions of the intermediate volatile organic compounds in both liquid and vapor phases.

(2) The switch from pure N_2 to a mixture of CO_2 and N_2 at 0.1 MPa led to a remarkable increase in the yield of produced gas at the expense of both the produced water and condensable organic compounds. This could be mainly due to the promotion of the thermal cracking of the volatile organic compounds at a high partial pressure of CO_2, which is also consistent with the measured higher yields of CH_4 and CO. The increased yield of CO can also be seen as a direct result of the enhanced reverse Boudouard reaction. However, increasing the absolute pressure can result in a promotion of the direct Boudouard reaction, leading to a higher production of CO_2 at the expense of CO.

(3) Interestingly, neither the pressure nor the pyrolysis atmosphere appeared to affect the yield of biochar for the range of operating conditions under consideration. Moreover, the potential stability of biochar's carbon was found to be similar, regardless of the operating parameters used. Nevertheless, a much higher porosity development (in terms of specific surface area and volume of ultra-micropores) was measured for the biochar produced at 0.1 MPa under an atmosphere of CO_2/N_2.

(4) We can conclude that, for the biomass feedstock used here at a pyrolysis peak temperature of 500 °C, using a mixture of CO_2 and N_2 (60:40 v/v) at atmospheric pressure is the most interesting way to simultaneously obtain a potentially recalcitrant and microporous biochar and an appropriate pyrolysis gas with relatively high contents of CH_4 and CO.

Acknowledgements

This project has received funding from the European Union's Horizon 2020 research and innovation programme under the Marie Skłodowska-Curie grant agreement No 721991. JJM also express his gratitude to the Aragon Government (GPT group) and the European Social Fund for additional financial support.

Appendix A. Supplementary data

Nomenclature

R_{50} = Harvey's recalcitrance index (−)

S_{BET} = Brunauer–Emmet–Teller specific surface area ($m^2\ g^{-1}$)

stable-C = mass fraction of C remaining after H2O2 oxidation (−)

TC# = temperatures measured by the thermocouples placed within the reactor (°C)

T_{max} = process temperature at which the highest devolatilization rate is attained (°C)

V_{DR} = limiting micropore volumes from the Dubinin-Radushkevich equation ($cm^3\ g^{-1}$)

V_{ultra} = ultra-micropore volume ($cm^3\ g^{-1}$)

$x_{FC,bc}$ = mass fraction of fixed-carbon in the biochar (daf basis)

y_{char} = mass yield of biochar in a dry and ash-free basis (−)

y_{FC} = fixed-carbon yield in a dry and ash-free basis (−)

y_{gas} = mass yield of produced gas in a dry and ash-free basis (−)

y_{org} = mass yield of condensable organics in a dry and ash-free basis (−)

y_{water} = mass yield of produced water in a dry and ash-free basis (−)

Acronyms

AAEMs = alkali and alkaline Earth metal species

DTG = differential thermogravimetric analysis

daf = dry-ash-free

GCMC = Grand Canonical Monte Carlo

GHSV = gas hourly space velocity (h^{-1})

PID = proportional integral derivative

WS = wheat straw

XRF = X-Ray Fluorescence spectroscopy

μ-GC = micro gas chromatograph

References

[1] F. Li, X. Cao, L. Zhao, J. Wang, Z. Ding, Effects of Mineral Additives on Biochar Formation: Carbon Retention, Stability, and Properties, Environ. Sci. Technol. 48 (2014) 11211–11217. https://doi.org/10.1021/es501885n.

[2] J.J. Manyà, Pyrolysis for Biochar Purposes: A Review to Establish Current Knowledge Gaps and Research Needs, Environ. Sci. Technol. 46 (2012) 7939–7954. https://doi.org/10.1021/es301029g.

[3] J. Lehmann, S. Joseph, Biochar for Environmental Management: An Introduction, in: J. Lehmann, S. Joseph (Eds.), Biochar Environ. Manag. Sci. Technol., Earthscan, London, 2009: pp. 1–10.

[4] J.J. Manyà, D. Alvira, M. Azuara, D. Bernin, N. Hedin, Effects of Pressure and the Addition of a Rejected Material from Municipal Waste Composting on the Pyrolysis of Two-Phase Olive Mill Waste, Energy Fuels 30 (2016). https://doi.org/10.1021/acs.energyfuels.6b01579.

[5] M. Azuara, E. Sáiz, J.A. Manso, F.J. García-Ramos, J.J. Manyà, Study on the effects of using a carbon dioxide atmosphere on the properties of vine shoots-derived biochar, J. Anal. Appl. Pyrolysis 124 (2017). https://doi.org/10.1016/j.jaap.2016.11.022.

[6] V. Dhyani, T. Bhaskar, A comprehensive review on the pyrolysis of lignocellulosic biomass, Renew. Energy 129 (2018) 695–716. https://doi.org/10.1016/j.renene.2017.04.035.

[7] W. Song, M. Guo, Quality variations of poultry litter biochar generated at different pyrolysis temperatures, J. Anal. Appl. Pyrolysis 94 (2012) 138–145. https://doi.org/10.1016/j.jaap.2011.11.018.

[8] O. Mašek, P. Brownsort, A. Cross, S. Sohi, Influence of production conditions on the yield and environmental stability of biochar, Fuel 103 (2013) 151–155. https://doi.org/10.1016/j.fuel.2011.08.044.

[9] F. Ronsse, S. van Hecke, D. Dickinson, W. Prins, Production and characterization of slow pyrolysis biochar: Influence of feedstock type and pyrolysis conditions, GCB Bioenergy 5 (2013) 104–115. https://doi.org/10.1111/gcbb.12018.

[10] J.J. Manyà, S. Laguarta, M.A. Ortigosa, J.A. Manso, Biochar from slow pyrolysis of two-phase olive mill waste: Effect of pressure and peak temperature on its potential stability, Energy Fuels 28 (2014) 3271–3280. https://doi.org/10.1021/ef500654t.

[11] L. Wang, M. Trninic, Ø. Skreiberg, M. Gronli, R. Considine, M.J. Antal, Is Elevated Pressure Required To Achieve a High Fixed-Carbon Yield of Charcoal from Biomass? Part 1: Round-Robin Results for Three Different Corncob Materials, Energy Fuels 25 (2011) 3251–3265. https://doi.org/10.1021/ef200450h.

[12] W.S.L. Mok, M.J. Antal Jr., Effects of pressure on biomass pyrolysis. I. Cellulose pyrolysis products, Thermochim. Acta 68 (1983) 155–164. https://doi.org/10.1016/0040-6031(83)80221-4.

[13] M.J. Antal, S.G. Allen, X. Dai, B. Shimizu, M.S. Tam, M. Grønli, Attainment of the theoretical yield of carbon from biomass, Ind. Eng. Chem. Res. 39 (2000) 4024–4031. https://doi.org/10.1021/ie000511u.

[14] M.J. Antal Jr., W.S.L. Mok, Review of Methods for Improving the Yield of Charcoal from Biomass, Energy Fuels 4 (1990) 221–225. https://doi.org/10.1021/ef00021a001.

[15] P. Rousset, C. Figueiredo, M. De Souza, W. Quirino, Pressure effect on the quality of eucalyptus wood charcoal for the steel industry: A statistical analysis approach, Fuel Process. Technol. 92 (2011) 1890–1897. https://doi.org/10.1016/j.fuproc.2011.05.005.

[16] E.S. Noumi, J. Blin, J. Valette, P. Rousset, Combined Effect of Pyrolysis Pressure and Temperature on the Yield and CO2Gasification Reactivity of Acacia Wood in macro-TG, Energy Fuels 29 (2015) 7301–7308. https://doi.org/10.1021/acs.energyfuels.5b01454.

[17] M.J. Antal, E. Croiset, X. Dai, C. DeAlmeida, W.S.L. Mok, N. Norberg, J.-R. Richard, M. Al Majthoub, High-Yield Biomass Charcoal, Energy Fuels 10 (1996) 652–658. https://doi.org/10.1021/ef9501859.

[18] J. Recari, C. Berrueco, S. Abelló, D. Montané, X. Farriol, Effect of temperature and pressure on characteristics and reactivity of biomass-derived chars, Bioresour. Technol. 170 (2014) 204–210. https://doi.org/10.1016/j.biortech.2014.07.080.

[19] Y. Qian, J. Zhang, J. Wang, Pressurized pyrolysis of rice husk in an inert gas sweeping fixed-bed reactor with a focus on bio-oil deoxygenation, Bioresour. Technol. 174 (2014) 95–102. https://doi.org/10.1016/j.biortech.2014.10.012.

[20] F. Melligan, R. Auccaise, E.H. Novotny, J.J. Leahy, M.H.B. Hayes, W. Kwapinski, Pressurised pyrolysis of Miscanthus using a fixed bed reactor, Bioresour. Technol. 102 (2011) 3466–3470. https://doi.org/10.1016/j.biortech.2010.10.129.

[21] J.J. Manyà, F.X. Roca, J.F. Perales, TGA study examining the effect of pressure and peak temperature on biochar yield during pyrolysis of two-phase olive mill waste, J. Anal. Appl. Pyrolysis 103 (2013) 86–95. https://doi.org/10.1016/j.jaap.2012.10.006.

[22] G. Pilon, J.-M. Lavoie, Pyrolysis of switchgrass (Panicum virgatum L.) at low temperatures within N2 and CO2 environments: Product yield study, ACS Sustain. Chem. Eng. 1 (2013) 198–204. https://doi.org/10.1021/sc300098e.

[23] A. Enders, K. Hanley, T. Whitman, S. Joseph, J. Lehmann, A. Whitman, S. Joseph, J. Lehmann, Characterization of biochars to evaluate recalcitrance and agronomic performance, Bioresour. Technol. 114 (2012) 644–653. https://doi.org/10.1016/j.biortech.2012.03.022.

[24] J.J. Manyà, M.A. Ortigosa, S. Laguarta, J.A. Manso, Experimental study on the effect of pyrolysis pressure, peak temperature, and particle size on the potential stability of vine shoots-derived biochar, Fuel 133 (2014) 163–172. https://doi.org/:10.1016/j.fuel.2014.05.019.

[25] J.J. Manyà, M. Azuara, J.A. Manso, Biochar production through slow pyrolysis of different biomass materials: Seeking the best operating conditions, Biomass Bioenergy 117 (2018) 115–123. https://doi.org/10.1016/j.biombioe.2018.07.019.

[26] K. Crombie, O. Masek, S.P. Sohi, P. Brownsort, A. Cross, The effect of pyrolysis conditions on biochar stability as determined by three methods, GCB Bioenergy 5 (2013) 122–131. https://doi.org/10.1111/gcbb.12030.

[27] O.R. Harvey, L.J. Kuo, A.R. Zimmerman, P. Louchouarn, J.E. Amonette, B.E. Herbert, An index-based approach to assessing recalcitrance and soil carbon sequestration potential of engineered black carbons (biochars), Environ. Sci. Technol. 46 (2012) 1415–1421. https://doi.org/10.1021/es2040398.

[28] A. Cross, S.P. Sohi, A method for screening the relative long-term stability of biochar, GCB Bioenergy 5 (2013) 215–220. https://doi.org/10.1111/gcbb.12035.

[29] L. Wang, O. Skreiberg, M. Gronli, G.P. Specht, M.J. Antal, Is elevated pressure required to achieve a high fixed-carbon yield of charcoal from biomass? Part 2: The importance of particle size, Energy Fuels 27 (2013) 2146–2156. https://doi.org/10.1021/ef400041h.

[30] C. Di Blasi, G. Signorelli, C. Di Russo, G. Rea, Product Distribution from Pyrolysis of Wood and Agricultural Residues, Ind. Eng. Chem. Res. 38 (1999) 2216–2224. https://doi.org/10.1021/ie980711u.

[31] A. Demirbas, Effects of temperature and particle size on bio-char yield from pyrolysis of agricultural residues, J. Anal. Appl. Pyrolysis 72 (2004) 243–248. https://doi.org/10.1016/j.jaap.2004.07.003.

[32] M. Azuara, B. Baguer, J.I. Villacampa, N. Hedin, J.J. Manyà, Influence of pressure and temperature on key physicochemical properties of corn stover-derived biochar, Fuel 186 (2016) 525–533. https://doi.org/10.1016/j.fuel.2016.08.088.

[33] L. Zhao, X. Cao, O. Mašek, A. Zimmerman, Heterogeneity of biochar properties as a function of feedstock sources and production temperatures, J. Hazard. Mater. 256–257 (2013) 1–9. https://doi.org/10.1016/j.jhazmat.2013.04.015.

[34] W. Suliman, J.B. Harsh, N.I. Abu-Lail, A.M. Fortuna, I. Dallmeyer, M. Garcia-Perez, Influence of feedstock source and pyrolysis temperature on biochar bulk and surface properties, Biomass Bioenergy 84 (2016) 37–48. https://doi.org/10.1016/j.biombioe.2015.11.010.

[35] A. V. McBeath, C.M. Wurster, M.I. Bird, Influence of feedstock properties and pyrolysis conditions on biochar carbon stability as determined by hydrogen pyrolysis, Biomass Bioenergy 73 (2015) 155–173. https://doi.org/10.1016/J.BIOMBIOE.2014.12.022.

[36] K.C. Kim, T.U. Yoon, Y.S. Bae, Applicability of using CO2 adsorption isotherms to determine BET surface areas of microporous materials, Microporous Mesoporous Mat. 224 (2016) 294−301. https://doi.org/10.1016/j.micromeso.2016.01.003.

[37] R. Ragucci, P. Giudicianni, A. Cavaliere, Cellulose slow pyrolysis products in a pressurized steam flow reactor, Fuel 107 (2013) 122–130. https://doi.org/10.1016/j.fuel.2013.01.057.

[38] F. Ateş, N. Miskolczi, B. Saricaoğlu, Pressurized pyrolysis of dried distillers grains with solubles and canola seed press cake in a fixed-bed reactor, Bioresour. Technol. 177 (2015) 149–158. https://doi.org/10.1016/j.biortech.2014.10.163.

[39] J. Lee, X. Yang, S.H. Cho, J.K. Kim, S.S. Lee, D.C.W. Tsang, Y.S. Ok, E.E. Kwon, Pyrolysis process of agricultural waste using CO2 for waste management, energy recovery, and biochar fabrication, Appl. Energy 185 (2017) 214–222. https://doi.org/10.1016/j.apenergy.2016.10.092.

[40] C. Guizani, F.J. Escudero-Sanz, S. Salvador, Effects of CO2 on biomass fast pyrolysis: Reaction rate, gas yields and char reactive properties, Fuel 116 (2014) 310–320. https://doi.org/10.1016/j.fuel.2013.07.101.

[41] J.H. Windeatt, A.B. Ross, P.T. Williams, P.M. Forster, M.A. Nahil, S. Singh, Characteristics of biochars from crop residues: Potential for carbon sequestration and soil amendment, J. Environ. Manage. 146 (2014) 189–197. https://doi.org 10.1016/j.jenvman.2014.08.003.

[42] W. Hao, E. Björkman, M. Lilliestråle, N. Hedin, Activated carbons prepared from hydrothermally carbonized waste biomass used as adsorbents for CO2, Appl. Energy 112 (2013) 526–532. https://doi.org 10.1016/j.apenergy.2013.02.028.

[43] J.J. Manyà, B. González, M. Azuara, G. Arner, Ultra-microporous adsorbents prepared from vine shoots-derived biochar with high CO2 uptake and CO2/N2 selectivity, Chem. Eng. J. 345 (2018) 631–639. https://doi.org 10.1016/j.cej.2018.01.092.

Table 1. Proximate, ultimate, and XRF analyses of the wheat straw pellets

Proximate (wt. %)	
Ash	3.67 ± 0.13
Moisture	6.60 ± 0.20
Volatile matter	77.7 ± 0.31
Fixed carbon	12.0 ± 0.18
Ultimate (wt. % in daf basis)	
C	49.0 ± 0.52
H	7.01 ± 0.04
N	0.704 ± 0.01
O	43.2[a]
Inorganic matter as equivalent oxides (wt. % of ash)[b]	
K_2O	53.2
CaO	17.4
SiO_2	16.9
P_2O_5	4.46
Al_2O_3	1.66
Cl (inorganic)	1.53
MgO	1.46
S (inorganic)	1.31
Fe_2O_3	1.14

[a] Oxygen was calculated by difference.

[b] Only listed components with a composition higher than 1%.

Table 2. Main reactions probably occurring during the release of the pyrolysis gas

No.	Reaction	Extent of reaction (ξ)[c] (kmol h^{-1})	
		500 °C and 0.1 MPa	500 °C and 0.5 MPa
1	$H_2O + CO \rightleftharpoons CO_2 + H_2$	0.390	0.390
2	$2CO \rightleftharpoons CO_2 + C$	0.937	0.972
3	$3H_2 + CO \rightleftharpoons CH_4 + H_2O$	0.614	0.825
4	$C + 2H_2 \rightleftharpoons CH_4$	0.343	0.693
5	$C + H_2O \rightleftharpoons CO + H_2$	−0.714	−0.871
6	$2H_2 + 2CO \rightleftharpoons CO_2 + CH_4$	0.706	0.867

[c] Calculated using Aspen Plus V8.8; NRTL package and a Gibbs Reactor module. Stoichiometric coefficients were taken as initial molar flow rates (in kmol h^{-1}) for all the species involved in the reaction.

Table 3. Main characteristics of the produced biochars

	Pyrolysis conditions			
	0.1_N_2	0.5_N_2	0.1_N_2&CO_2	0.5_N_2&CO_2
Proximate analysis (wt. % in dry basis)				
Ash	12.8 ± 0.20	11.7 ± 0.14	13.1 ± 0.16	13.3 ± 0.03
Volatile matter	25.0 ± 0.65	18.3 ± 0.16	26.3 ± 1.78	25.7 ± 1.13
Fixed carbon	62.1 ± 0.42	70.0 ± 0.14	60.6 ± 1.83	61.0 ± 1.08
Ultimate analysis (wt. % in daf basis)				
C	86.0 ± 0.02	85.0 ± 0.13	87.7 ± 0.07	89.3 ± 0.13
H	3.87 ± 0.03	3.31 ± 0.15	3.66 ± 0.01	3.30 ± 0.22
N	1.82 ± 0.01	1.89 ± 0.01	1.93 ± 0.01	2.09 ± 0.02
O[d]	8.30	9.77	6.66	5.28
Other				
y_{FC}[e]	0.199	0.231	0.202	0.205
Molar H:C ratio	0.539	0.468	0.500	0.443
Molar O:C ratio	0.072	0.086	0.060	0.044
S_{BET} ($m^2 \cdot g^{-1}$)	200	196	380	226
Pore volume (V_{DR}; $cm^3\ g^{-1}$)	0.112	0.110	0.197	0.129
Pore volume (V_{DFT}; $cm^3\ g^{-1}$)	0.0814	0.0839	0.150	0.0962

[d] Calculated by difference.

[e] Fixed-carbon yield calculated according to Eq. 1.

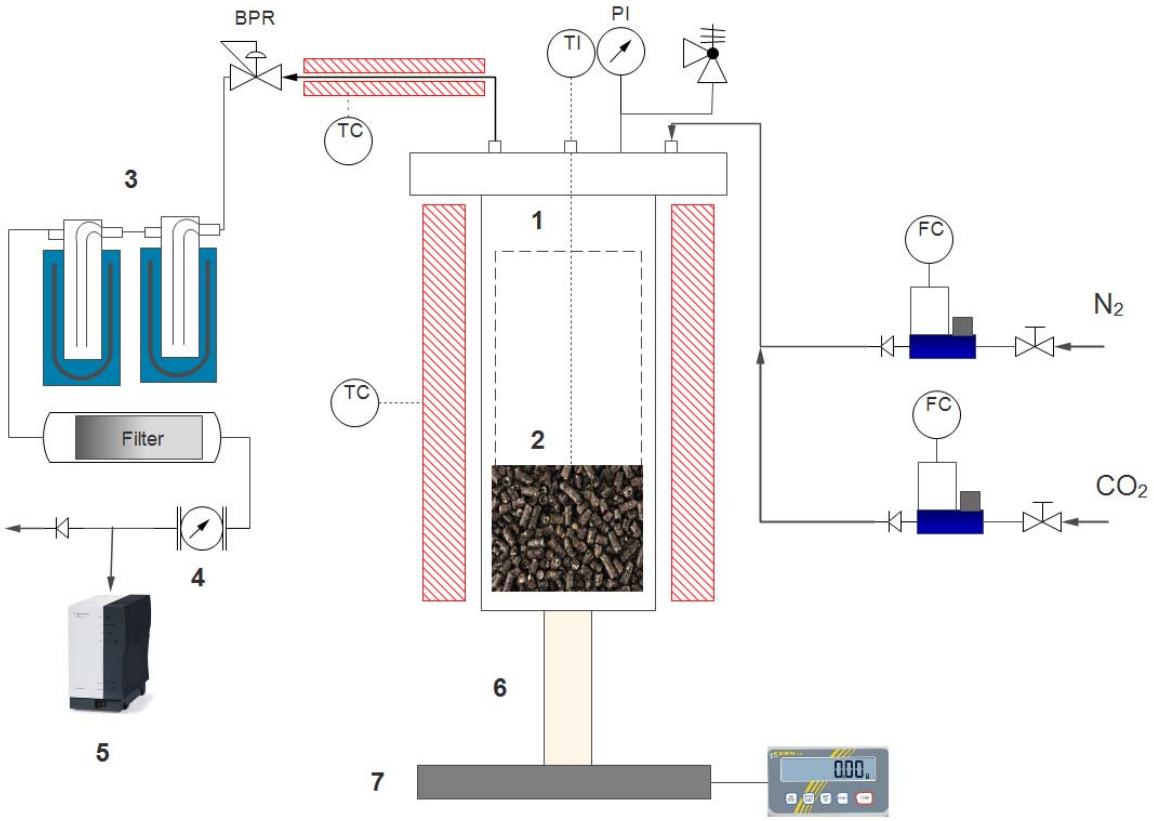

Fig. 1. Schematic layout of the pyrolysis device: (1) pyrolysis reactor, (2) biomass bed, (3) condensation system, (4) volumetric gas meter, (5) micro-GC, (6) ceramic tube, and (7) weighing platform.

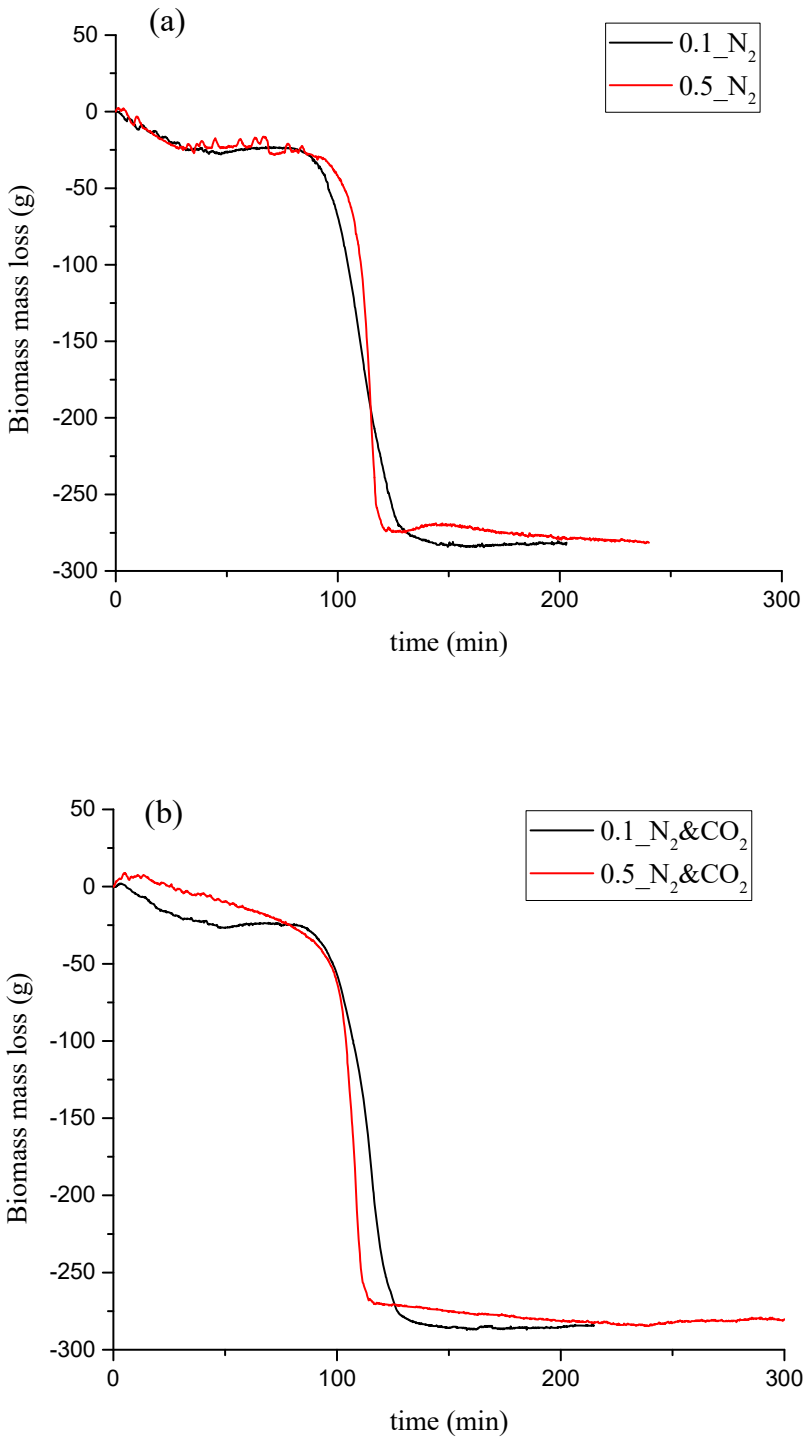

Fig. 2. A comparison between the mass-loss evolutions along the pyrolysis process at 0.1 MPa and 0.5 MPa, using (a) a N_2 atmosphere, and (b) a CO_2/N_2 environment.

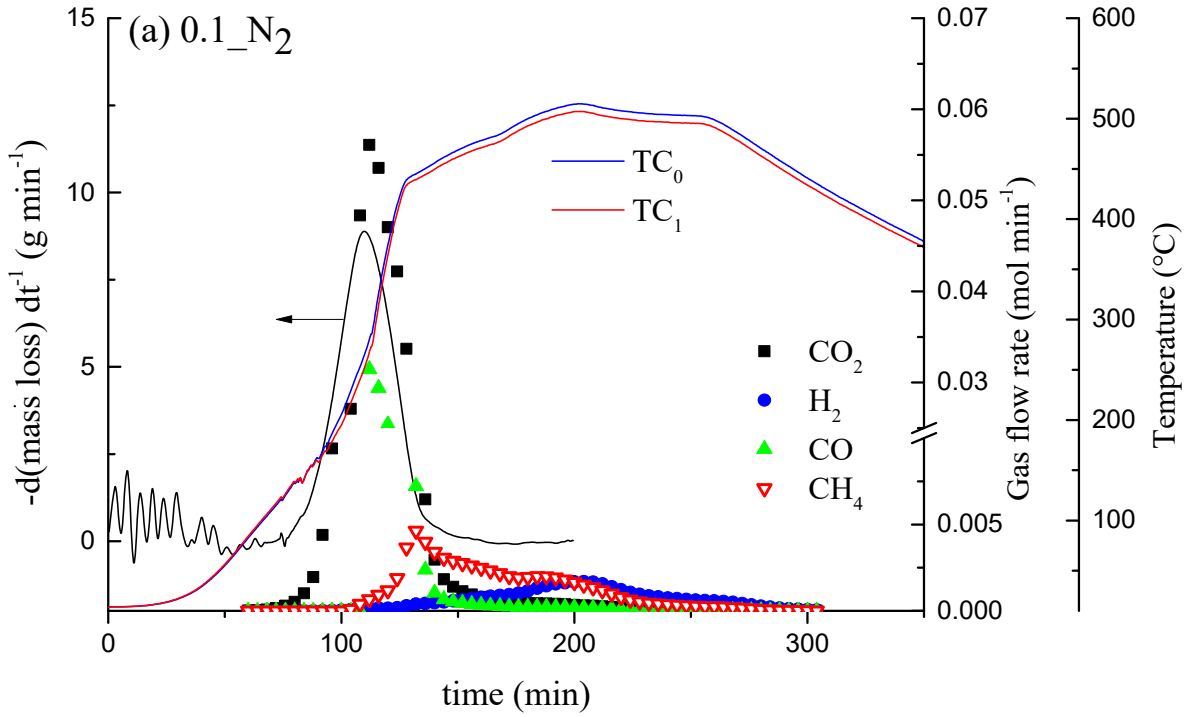
(a) 0.1_N2
-d(mass loss) dt-1 (g min-1)
Gas flow rate (mol min-1)
Temperature (°C)
time (min)
TC0
TC1
CO2
H2
CO
CH4

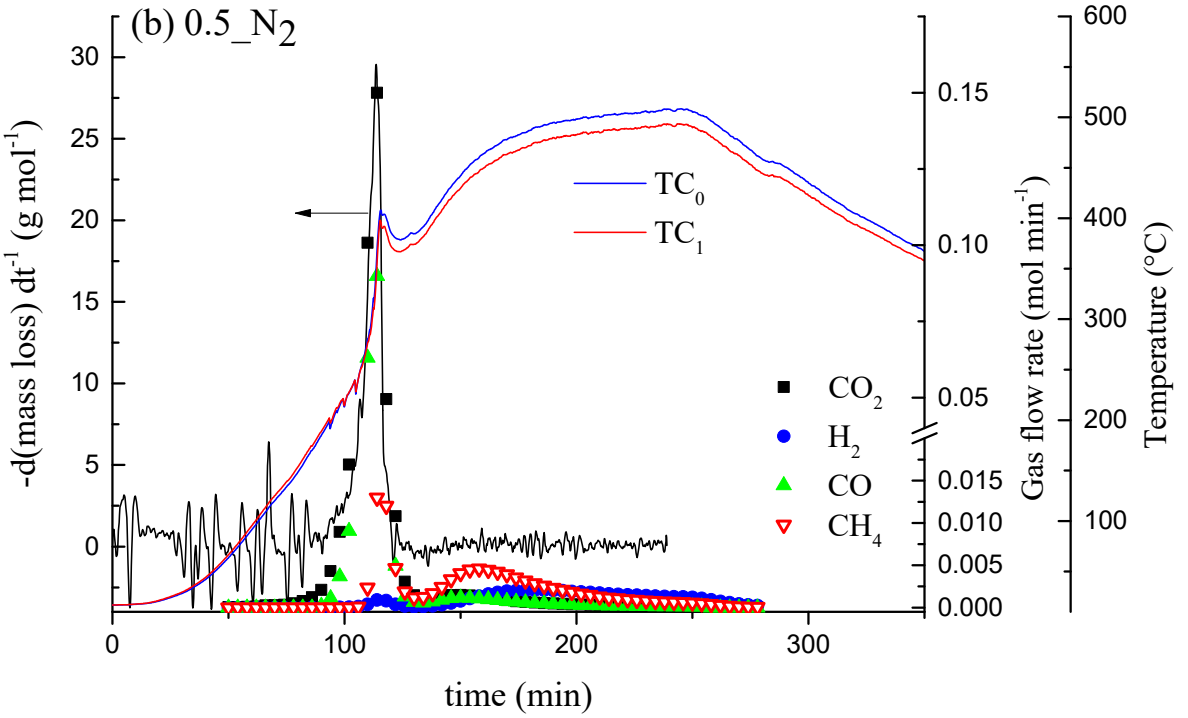
(b) 0.5_N2
-d(mass loss) dt-1 (g mol-1)
Gas flow rate (mol min-1)
Temperature (°C)
time (min)
TC0
TC1
CO2
H2
CO
CH4

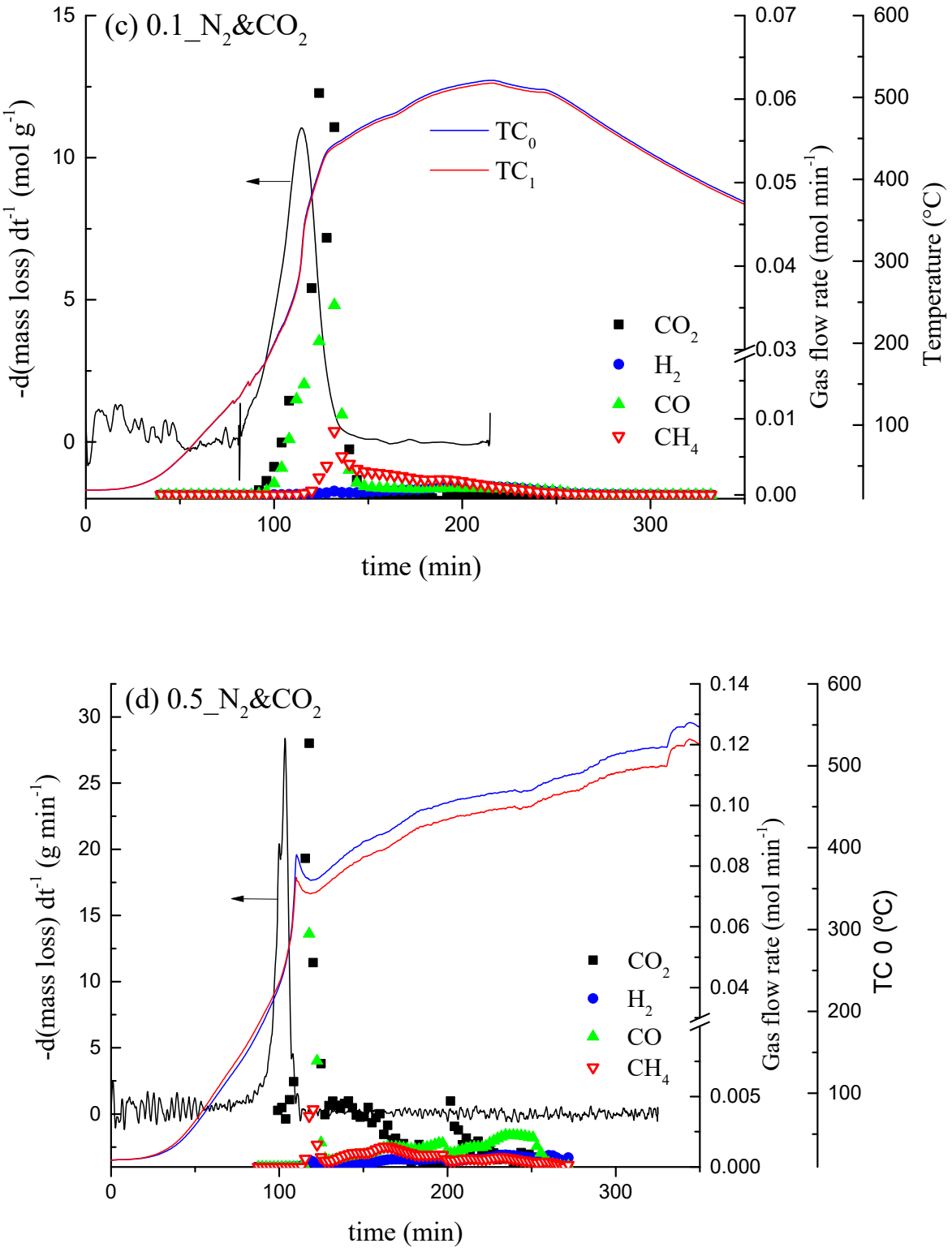

Fig. 3. Time derivative of the mass loss, evolution of temperatures within the bed (TC_0 and TC_1), and molar flows of the main gaseous species released during the pyrolysis process (produced CO_2, CO, CH_4, and H_2) for experiments conducted at 0.1 MPa under N_2 (a), 0.5 MPa under N_2 (b), 0.1 MPa using a mixture CO_2/N_2 (c), and at 0.5 MPa using a mixture CO_2/N_2 (d).

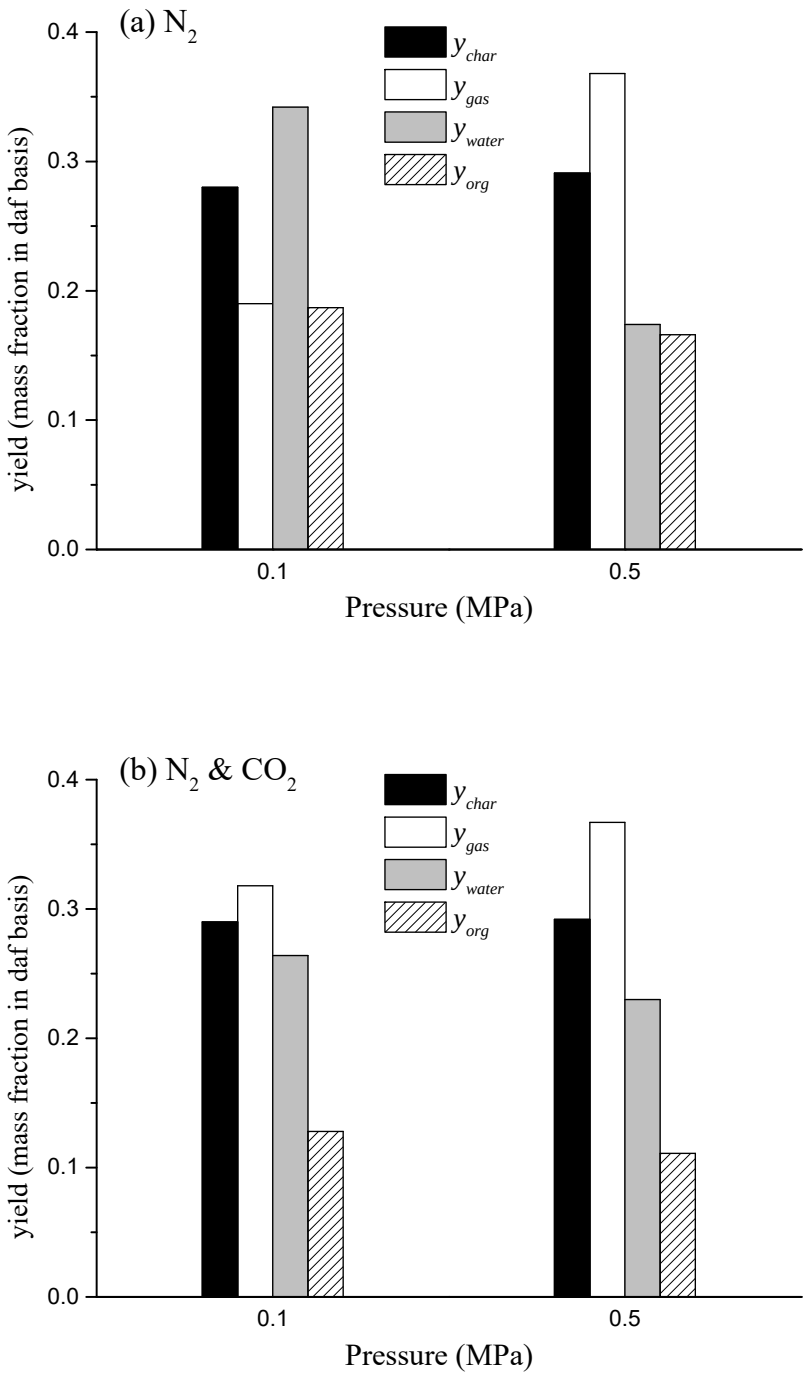

Fig. 4: Mass yields (in a daf basis) of biochar (y_{char}), produced water (y_{water}), organics (y_{org}), and gas (y_{gas}) as a function of the absolute pressure: (a) pyrolysis runs conducted under pure N_2, (b) runs conducted within a CO_2/N_2 environment.

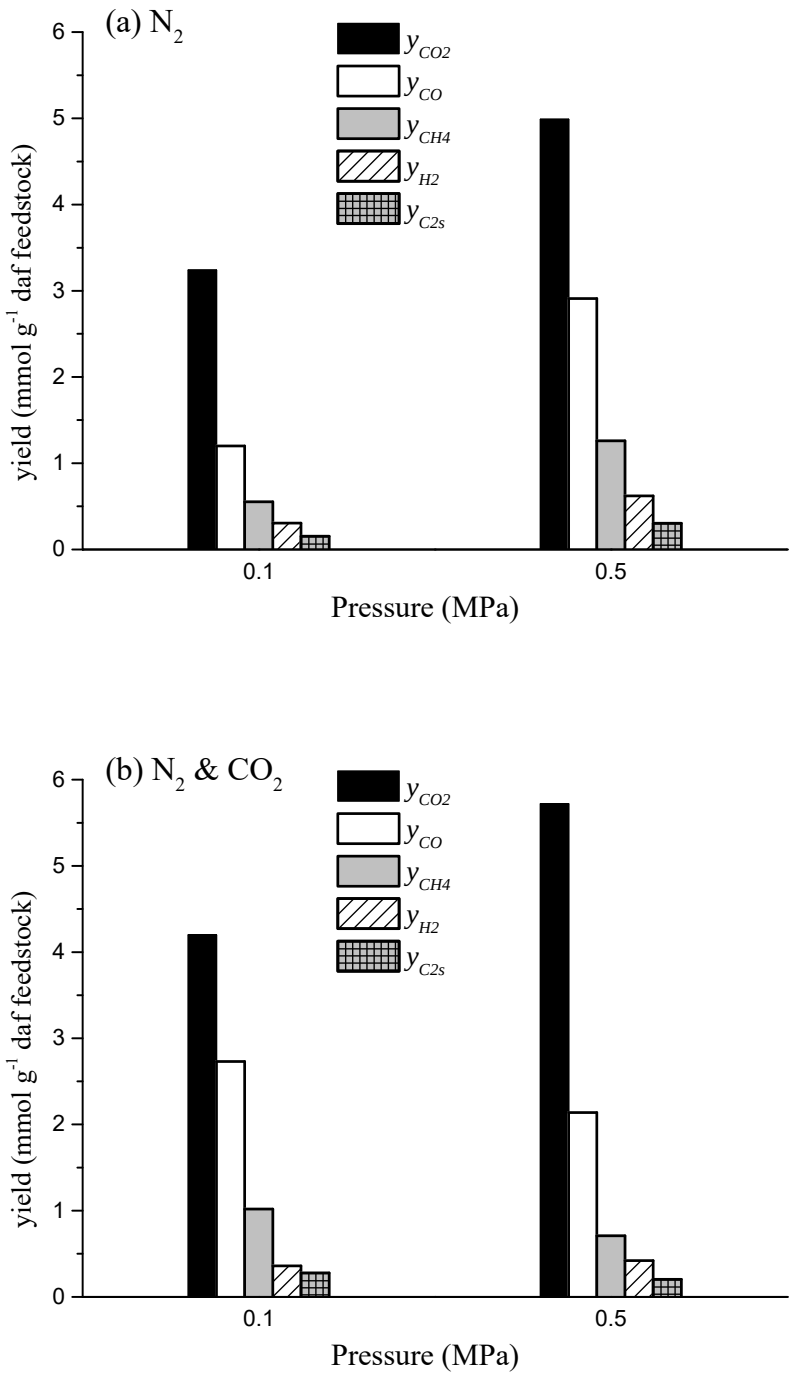

Fig. 5. Cumulative yields of the main gaseous compounds (mmol g^{-1} of daf feedstock) as a function of the absolute pressure: (a) pyrolysis runs conducted under pure N_2, (b) runs conducted within a CO_2/N_2 environment.

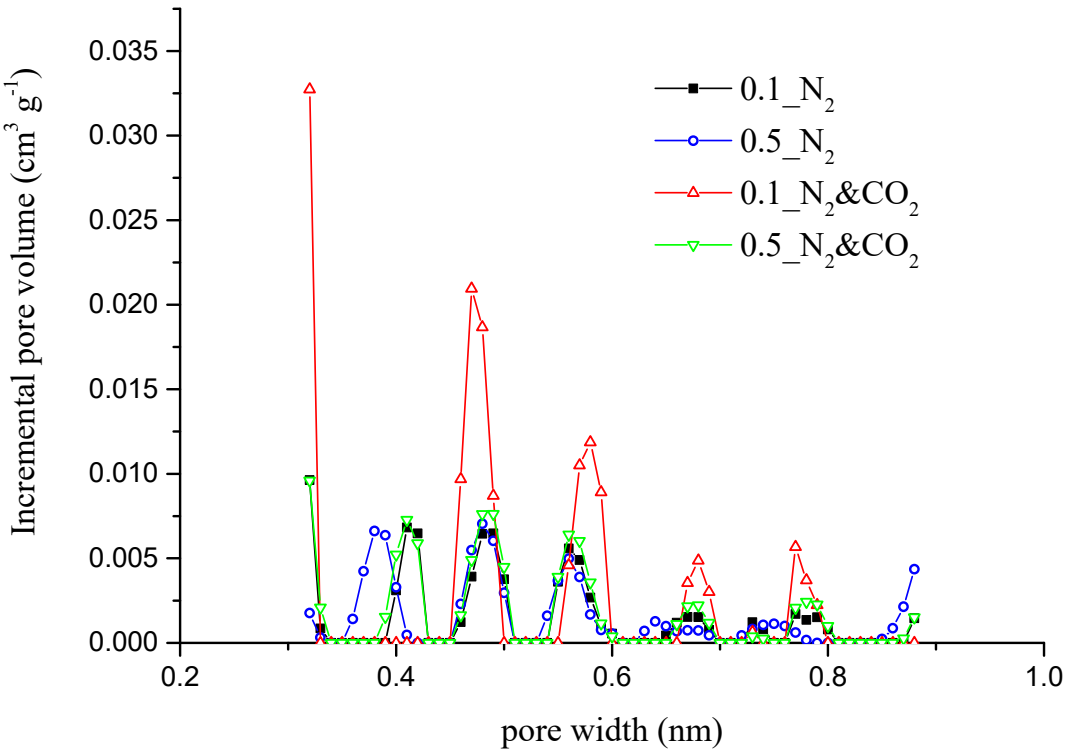

Fig. 6. Pore size distributions for the biochars obtained under different operating conditions (see legend) deduced from the CO_2 adsorption isotherms at 0 °C.